of possible trip times and in some cases reduces the required propulsive velocity increment

2) The use of an atmospheric turn at Mars can reduce the required propulsive velocity increment to a value approaching that for a one-way transfer to Mars, depending on the feasible vehicle lift-drag ratios Low propulsive velocity increments occur for trip times down to about 1 year

3) In general, greater propulsive velocity increments are required in 1980 than in 1971 The propulsive velocity increments for the atmospheric-turn trajectories are the least affected by the launch year

4) The propulsive-gravity and the atmospheric-turn trajectories appear to offer the potential of fast, light weight, nonstop round trips to Mars

Reference

[1] Knip, G, Jr and Zola, C L, "Three dimensional trajectory analysis for round trip missions to Mars," NASA TN D-1316 (1962)

Nonlinear Pressure Coupling in Cylindrical Shell Analysis

PAUL E WILSON* AND EDWARD E SPIER†
General Dynamics/Astronautics, San Diego, Calif

Nomenclature

a	= radius of shell middle surface
A B	= constants of integration
D	= flexural rigidity, $Eh^3/12(1-\nu^2)$
E	= modulus of elasticity
h	= shell thickness
i	= $(-1)^{1/2}$
k	= shell parameter, Eh/a^2
m	= nondimensional load parameter
M_0,Q_0	= moment and shear at discontinuity neglecting $N_x(d^2w/dx^2)$
M_N,Q_N	= moment and shear at discontinuity including $N_x(d^2w/dx^2)$
N_x	= axial stress resultant, positive when tensile
p	= internal pressure
w	= radial deflection measured positive inward
w_c,w_p	= complementary and particular solutions, respectively
x	= axial coordinate
$\alpha,\beta,\bar{\beta},\gamma$	= parameters entering into complementary solution
δ_1,δ_2	= membrane expansions given by Eq (7)
η	= shell thickness ratio, h_1/h_2
λ^4	= shell parameter, $k/4D$
ν	= Poisson's ratio

Introduction

MANY structural problems in the aerospace industry involve highly pressurized shells with large radius-thickness ratios, and under these circumstances, as suggested by Hetenyi,[1] the coupling effects of pressure often have a significant influence on discontinuity shears, moments, and stresses Accordingly, a number of investigations have recently been focused on this problem for pressurized cylindrical,[2–8] spherical,[9,10] and arbitrary shells of revolution [11] For internally pressurized shells, comparisons made between discontinuity analyses that include and neglect the coupling effects of meridional load[7,8] imply that use of the refined method generally yields lower calculated maximum stresses and results in a lighter-weight structure

Received October 30, 1963 This note summarizes results of one phase of research that was sponsored by General Dynamics/Astronautics under Research Program No 111-9372 The authors extend their appreciation to D R Cropper and others at General Dynamics/Astronautics for assisting in the preparation of this note

* Design Specialist, Structures Research Group

† Design Specialist, Structures Research Group Member AIAA

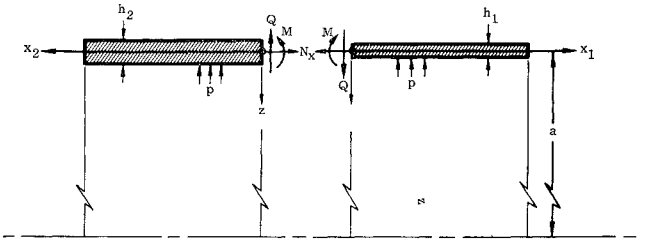

Fig 1 Shell juncture

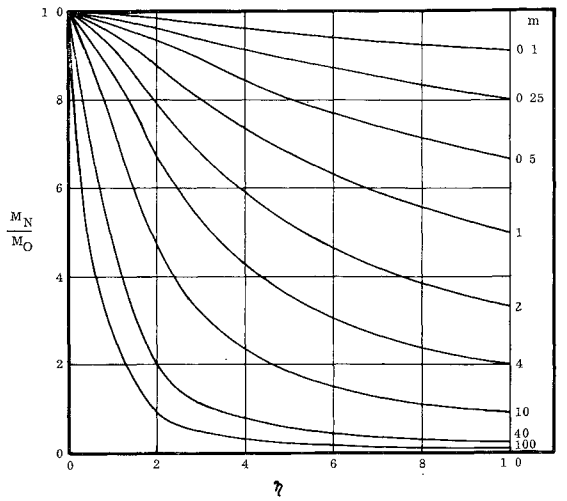

Fig 2 Moment comparison curves

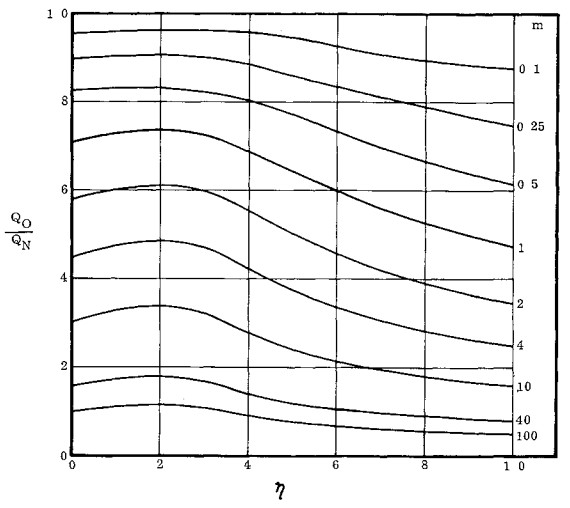

Fig 3 Shear comparison curves

In this note, two well-known thin shell theories are used to evaluate and compare shears and moments at the juncture of two pressurized cylindrical shells For highly pressurized cylinders with large radius-thickness ratios, the numerical results indicate that nonlinear coupling effects of pressure significantly influence computed values of discontinuity shears and moments

Theory

The differential equation that governs small axisymmetric displacements of thin cylindrical shells may be written in the form[12]

$$D\frac{d^4w}{dx^4} - N_x\frac{d^2w}{dx^2} + \frac{Eh}{a^2}w = -p + \nu\frac{N_x}{a} \qquad (1)$$

In many discontinuity analyses[13] it is permissible, as verified by test results,[14 15] to delete the pressure coupling term $N_x(d^2w/dx^2)$ from Eq (1) However, by parametric evaluation of a simple problem, it will be demonstrated that this simplification process is not generally valid for highly pressurized cylindrical shells with large radius-thickness ratios

The general solution of Eq (1) for a semi-infinite cylindrical shell is well known[1] and may be expressed in the form

$$w = w + w_p \tag{2}$$

where

$$w_p = -\frac{a^2}{Eh}\left(p - \nu\frac{N_x}{a}\right) \tag{3}$$

$$\begin{aligned} N_x < 2(kD)^{1/2} \qquad & w = e^{-\alpha x}(A\sin\beta x + B\cos\beta x) \\ N_x = 2(kD)^{1/2} \qquad & w = e^{-\gamma x}(A + Bx) \\ N_x > 2(kD)^{1/2} \qquad & w = e^{-\alpha x}(A\sinh\bar{\beta}x + B\cosh\bar{\beta}x) \end{aligned} \tag{4}$$

and

$$\begin{aligned} \alpha &= \left(\lambda^2 + \frac{N_x}{4D}\right)^{1/2} \\ \beta = -i\bar{\beta} &= \left(\lambda^2 - \frac{N_x}{4D}\right)^{1/2} \\ \gamma &= \left(\frac{N_x}{2D}\right)^{1/2} \end{aligned} \tag{5}$$

Analysis

Figure 1 shows a longitudinal section of the juncture of two semi-infinite cylindrical shells that are subjected to internal pressure p Take $h_1 \leq h_2$ and let x_1 and x_2 be directed as shown With the compatibility and equilibrium conditions at the juncture, along with Eqs (2–5), it may be shown that the discontinuity moment M_N and shear Q_N act as shown in Fig 1 and can be expressed in the following form:

$$\begin{aligned} M_N &= \frac{2D_1D_2\lambda_1^2\lambda_2^2(D_2\lambda_2^2 - D_1\lambda_1^2)(\delta_1 - \delta_2)}{(D_1\lambda_1^2 + D_2\lambda_2^2)^2 + 2D_1D_2\alpha_1\alpha_2(\lambda_1^2 + \lambda_2^2) + (N_x/2)(D_1\lambda_1^2 + D_2\lambda_2^2)} \\ Q_N &= \frac{4D_1D_2\lambda_1^2\lambda_2^2[\alpha_1\lambda_2^2D_2 + \alpha_2\lambda_1^2D_1 + (N_x/2)(\alpha_1 + \alpha_2)](\delta_1 - \delta_2)}{(D_1\lambda_1^2 + D_2\lambda_2^2)^2 + 2D_1D_2\alpha_1\alpha_2(\lambda_1^2 + \lambda_2^2) + (N_x/2)(D_1\lambda_1^2 + D_2\lambda_2^2)} \end{aligned} \tag{6}$$

where

$$\begin{aligned} \delta_i &= \frac{a^2}{Eh_i}\left(p - \nu\frac{N_x}{a}\right) \qquad i = 1, 2 \\ N_x &= pa/2 \end{aligned} \tag{7}$$

and the subscript i ($i = 1, 2$) denotes quantities evaluated in the region $0 \leq x_i \leq \infty$ When written in their present form, Eqs (6) are valid for all values of N_x

If effects of pressure coupling are neglected, the moment M_0 and shear Q_0 at the discontinuity may, by suitable reduction of Eqs (6), be shown to be

$$\begin{aligned} M_0 &= \frac{2D_1D_2\lambda_1^2\lambda_2^2(D_2\lambda_2^2 - D_1\lambda_1^2)(\delta_1 - \delta_2)}{(D_1\lambda_1^2 + D_2\lambda_2^2)^2 + 2D_1D_2\lambda_1\lambda_2(\lambda_1^2 + \lambda_2^2)} \\ Q_0 &= \frac{4D_1D_2\lambda_1^3\lambda_2^3(D_1\lambda_1 + D_2\lambda_2)(\delta_1 - \delta_2)}{(D_1\lambda_1^2 + D_2\lambda_2^2)^2 + 2D_1D_2\lambda_1\lambda_2(\lambda_1^2 + \lambda_2^2)} \end{aligned} \tag{8}$$

Equations (8) agree with results given earlier by Johns [13 14]

An interesting quantitative comparison of these results may be obtained by forming the dimensionless ratios (M_N/M_0) and (Q_0/Q_N) as follows:

$$\begin{aligned} \frac{M_N}{M_0} &= \frac{(1 + \eta^2)^2 + 2\eta^{3/2}(1 + \eta)}{(1 + \eta^2)^2 + 2\eta^{3/2}(1 + \eta)[(1 + m)(1 + m\eta^2)]^{1/2} + 2m\eta^2(1 + \eta^2)} \\ \frac{Q_0}{Q_N} &= \frac{1 + \eta^{5/2}}{(1 + 2m\eta^2)(1 + m)^{1/2} + \eta^{5/2}(1 + 2m)(1 + m\eta^2)^{1/2}}\,\frac{M_0}{M_N} \end{aligned} \tag{9}$$

where

$$\eta = \frac{h_1}{h_2} \qquad m = \frac{[3(1 - \nu^2)]^{1/2}}{2}\,\frac{pa^2}{Eh_1^2} \tag{10}$$

Plots of M_N/M_0 and Q_0/Q_N vs η for various values of the nondimensional load parameter m are shown in Figs 2 and 3, respectively Note that results obtained including effects of N_x on local bending imply that computed values of the discontinuity bending moment and shear are significantly reduced and increased, respectively, over corresponding values obtained by neglecting pressure coupling effects For example, consider the following case: $a = 20$ in ; $h_1 = 0\ 10$ in ; $h_2 = 0\ 20$ in ; $p = 200$ psi; $E = 10 \times 10^6$ psi; and $\nu = 0\ 3$ Thus, $\eta = 0\ 5$, $m = 0\ 661$, and, from Figs 2 and 3 $M_N = 0\ 75\ M_0$ and $Q_N = 1\ 39\ Q_0$ Consequently, in this instance the discontinuity moments and shears computed by neglecting coupling effects of meridional load are in error by approximately 25 and 39%, respectively

The stresses have not been discussed in this brief note However, preliminary calculations indicate that the maximum stress always occurs in the thinner shell For small values of η the longitudinal stress governs the design, whereas for large values of η the hoop stress governs Also, it was found that computed values of the maximum stress are reduced when pressure coupling effects are included in the analysis In practice it is recommended that the maximum stress be computed by using Eqs (6) in conjunction with the techniques outlined by Grossman[7] and Smith [8]

References

[1] Hetenyi, M , *Beams on Elastic Foundation* (University of Michigan Press, Ann Arbor, Mich (1946), 4th ed , Chap VI, pp 127–140

[2] Bijlaard, P P , "Stresses from radial loads and external moments in cylindrical pressure vessels," Welding J , Res Suppl , 608–617 (1955)

[3] Short, R D and Bart, R , "Analysis for determining stresses in stiffened cylindrical shells near structural discontinuities," David Taylor Model Basin Rept 1065 (1959)

[4] Pulos, J G and Salerno, V L , "Axisymmetric elastic deformations and stresses in a ring-stiffened perfectly circular cylindrical shell under external hydrostatic pressure," David Taylor Model Basin Rept 1497 (1961)

[5] Wei, B C F "Structural analysis of solid propellant rocket casings, ' ARS Preprint 1590-61 (1961)

[6] Greenbaum, G A "Effect of axial force on influence coefficients for thin cylindrical shells," M S Thesis, Dept Eng , Univ Calif Los Angeles (1961)

[7] Grossman, W B , "Investigation of maximum stresses in long pressurized cylindrical shells," AIAA J **1**, 1129–1132 (1963)

[8] Smith, G W , "Analysis of multiple discontinuities in shells of revolution including coupled effects of meridional load," General Dynamics/Astronautics Rept 63-0044, 7090 Program 3019 (1963)

[9] Bijlaard, P P "Computation of stresses from local loads in spherical pressure vessels " Welding Res Council, Bull 34, New York (1957)

[10] Cline, G B , "Effect of pressure-stress coupling upon the

influence coefficients of spherical shells,' Am Soc Mech Engrs Paper 62-WA-58 (1962)

[11] Nachbar, W, "Discontinuity stresses in pressurized thin shells of revolution,' Lockheed Missiles and Space Div, LMSD-48483 (1957)

[12] Timoshenko, S P, *Theory of Elastic Stability* (McGraw-Hill Book Co, Inc, New York (1936) Chap VII, pp 423–425

[13] Johns, R H and Orange, T W, "Theoretical elastic stress distributions arising from discontinuities and edge loads in several shell-type structures,' NASA TR R-103 (1961)

[14] Johns, R H, Morgan, W C, and Spera, D A, "Theoretical and experimental analysis of several typical junctions in space vehicle shell structures' ARS Preprint 2427-62 (1962)

[15] Morgan, W C and Bizon, P T, "Experimental investigation of stress distributions near abrupt change in wall thickness in thin-walled pressurized cylinders,' NASA TN (to be published)

Method for Determination of Velocity Distribution in a Thin Liquid Film

S L Persson*

Flygmotor Aeroengine Company, Trollhattan, Sweden

In conjunction with an investigation of film cooling of blunted bodies, a method has been developed for the measurement of the velocity distribution in thin liquid films The mean velocity and the thickness of the film are also determined Results are presented from measurements in water films with thicknesses of the order of 0 1 to 0 9 mm It is assumed that the suggested method also may find application in different types of boundary-layer investigations

FILM cooling has been suggested and applied as a means of protecting motor parts and aerodynamic bodies in high-temperature environments Different studies of film cooling with liquids have been reported [1–4] It is obvious from the results of these investigations that knowledge of the physics of the liquid film is of great importance to the designer of a film cooling system In particular, the stability of the film has a profound influence on the coolant efficiency

A method to measure the velocity profile in a thin liquid film (0 1 to 1 mm thick) has been developed A liquid film is generated on a plane surface from a slot injector Small metal particles are mixed uniformly with the liquid before the injection The film is photographed from above with a camera with well-known exposure time The length of the traces on the picture are proportional to the velocity of the particles The picture does not, however, reveal directly whether a certain particle has been traveling at the bottom of the film, close to the solid surface, or at the top, close to the air boundary layer

To obtain the velocity distribution, the following steps are taken First, a large number of particle traces, say 100, are measured at identical conditions Since the number of traces on each photograph is limited to around 20 (to avoid colliding traces), this means that the exposures must be repeated in short intervals (1 sec) Two assumptions are then made One is that the particle density in the liquid flow is uniform, that is, each cubic centimeter of liquid contains the same number of particles A special mixer before the injection slot is used to guarantee the uniform distribution The other assumption is that the velocity profile is monotonic The last assumption limits the use of the method to certain types of films It is not, however, considered to be a serious limitation to films pertinent to film-cooling practice

Received October 31, 1963

* Head, Physics Section, Research Department

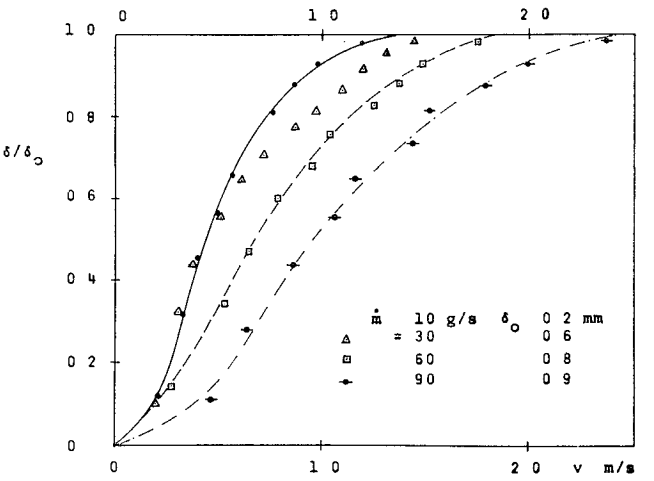

Fig 1 Velocity profiles in water film

After measurement of the traces, a diagram can be drawn over the number of particles as a function of the particle velocities Suppose that just 100 particles are measured Then, from the foregoing assumptions, it follows that the 10 particles with the highest velocity must travel in the film layer closest to the surface between air and liquid The next 10 particles will travel in the following layer, and so on The widths of these 10 layers are not equal but are proportional to the respective velocities due to the continuity principle The total film thickness can be calculated since the mass flow of liquid is known A mean velocity can also be determined

The apparatus that has been used consists of a mercury lamp for illumination of the particles and a camera The lamp was mounted so that the light rays, when hitting the particles, made as small an angle as possible with the film plane The camera, mounted perpendicular to the film plane, used an exposure time around 1 msec

In most of the experiments, nearly spherical aluminium particles with the diameters between 20 and 40 μm have been used These diameters are considered small enough to give a correct picture of the velocity profile ($d = \frac{1}{10}$ of the film thickness) Calculations have been made which show that particles that are incidentally halted at the slot have the right velocity at the test area if the particles are smaller than 0 1 mm

In Fig 1 are shown some results from the investigation Velocity profiles are given as a function of a dimensionless distance (distance from solid surface toward the interface divided by film thickness) The water mass flow was varied between 10 and 90 g/sec The film thicknesses are given All results presented in Fig 1 refer to tests with no outside air flow

Some tests have been made with an air flow blowing along the water surfaces In the tests hitherto made, no influence on the film velocity profile from the air flow has been observed No tests have been performed, however, at air velocities higher than 30 m/sec ($Re_x = 2 \times 10^5$)

The film thickness has been measured also with a separate method, using a needle that has been held close to the water surface Afterwards the distance between the needle point and the surface was measured The following measured thicknesses show the good agreement between the needle d_0 and the particle technique d:

$\dot{m} = 30$ g/sec	50 g/sec
$d = 0\ 37$	0 56 with air (50 m/sec)
$d = 0\ 37$	0 56 without air
$d_0 = 0\ 35$	0 50 without air

Other results from the preliminary investigations are given in Ref 4